EFFECTS OF FIBRE FAILURE AND INITIAL NOTCH SIZE ON THE FATIGUE CRACK GROWTH BEHAVIOUR OF A Tiβ21s/SCS-6 COMPOSITE

J. Liu and P. Bowen*

Fatigue crack growth in an 8-ply Tiβ21s/SCS-6 composite has been studied with particular emphasis on the effects of fibre failure and initial notch size (a_0/W). Acoustic emission (AE) has been used to detect fibre failure. A simple fibre bridging model has been used to interpret the results of fatigue crack growth in specimens with different initial notch sizes. The results show that the failure of fibres has a dominant role in determining whether the fatigue crack will eventually arrest. A smaller initial notch depth is often more damaging than a larger one when tested under an identical initial stress intensity factor range.

INTRODUCTION

Silicon carbide fibre reinforced titanium matrix composites (TMCs) are regarded as attractive candidates for use in aerospace applications at elevated temperatures (1). Their fatigue properties, which are important for such applications, have been studied extensively (1-11), and it is found that the intact fibres in the wake of fatigue crack can bridge the crack and decrease the crack growth driving force so that the TMCs can sustain much higher loads than the unreinforced matrix alloys. However, several studies have been carried out on the fatigue crack growth behaviour of TMCs with fibre failure being taken into account (1,7,8,10,11), and have found that the resistance of the composites will diminish once intact bridging fibres fail. Since the fibre failure in TMCs during fatigue is influenced not only by the maximum applied load, but also by the specimen geometry, and quite possibly by the precise loading history, careful studies are needed to address this topic.

The aim of this paper is to study the effects of fibre failure on the fatigue crack growth behaviour in a Tiβ21/SCS-6 composite. The effect of initial notch size on fibre failure and crack growth behaviour of the composite is also examined.

*IRC for High Performance Materials/School of Metallurgy and Materials,
The University of Birmingham, Edgbaston, Birmingham B15 2TT, UK

EXPERIMENTAL

The composite material used in this study is an 8-ply SCS-6 fibre reinforced Tiβ21s composite produced by Textron (USA) using the foil-fibre-foil procedure. The fibre volume fraction is 35%. Specimens used for these present three-point-bending fatigue tests are 75 mm long, 4 mm wide, and 1.8 mm thick. Notches of thickness ~0.2 mm and ~0.4 mm are introduced by diamond blade cutting and electrical discharge machining (EDM), respectively. The size of the notches varies from 0.2 to 1 mm (corresponding to a_0/W ratios of 0.05 to 0.25, and where a_0 is the initial notch depth, and W is the test piece width).

Fatigue tests were conducted on a 10 kN Instron servo-hydraulic testing system under load control at a load ratio of 0.5 and at a frequency of 10 Hz. The initial applied stress intensity factor range, ΔK_0, was in all cases here controlled to be approximately 17 MPa$\sqrt{m}$ (and are calculated by assuming that the cut notch can be treated approximately as a sharp pre-crack). The crack extension was monitored continuously using the direct current potential drop (DCPD) technique so that the sudden changes in crack growth rate as a result of fibre failure can be detected. The direct current provided by a stable current source was adjusted to give an initial potential across the notch of 1.0 mV.

To monitor the fibre failure during fatigue, an acoustic emission (AE) sensor with a resonant frequency of 300 kHz was attached to the specimen at a position located approximately 10 mm away from the notch. The AE signals were amplified and analysed by a PAC Locan Jr. The gain of the preamplifier was set to 40 dB, and the internal gain and threshold was set to 20 and 68 dB, respectively.

RESULTS AND DISCUSSION

Characterisation of Fibre Failure Using AE

The amplitude of the AE signals is useful to distinguish the signals caused by the fibre failure from those caused by other events, such as matrix deformation and interfacial sliding. When the cumulative hits of AE signals are plotted against the amplitude under the condition employed here, a gap can be found at approximately 90 to 92 dB (Fig.1(a)), and above which the signals are caused by fibre failure. The signals caused by fibre failure also have much higher energy than those deriving from other events (Fig.1(b)).

Fatigue Crack Growth Behaviour

Effects of fibre failure. The effect of fibre failure on the fatigue crack growth behaviour of the composite can be well characterised by using both PD and AE techniques. As shown in Fig.2, the crack growth rate, da/dN, tends to decrease with the number of cycles because the bridging length tends to increase with the crack length. However, whenever fibre failure is detected, sudden increases in da/dN are observed.

Another point of interest in Fig.2 is that if fatigue tests are continued after what has been considered in much other work to be crack arrest (i.e., $da/dN \leq 10^{-8}$ mm/cycle), da/dN may subsequently increase again and lead to the eventual failure of the specimen as a result of fibre failure. This implies that the fibre strength may be degraded by repeated cyclic loading. It has been observed that fatigue loading can damage the fibre coating (7).

Whether the degradation in fibre strength is caused by damage to the fibre coating and/or by damage to the fibre itself needs further study.

Effects of initial notch size. The effects of initial notch size on fatigue behaviour are listed in TABLE 1, and typical variations of da/dN with crack length, a, are shown in Fig.3. For specimens with a large a_0/W (~0.25), da/dN tends to decrease as a increases (sometimes a slight increase in da/dN is observed at the very beginning of the test after crack initiation from the cut notch). Although sudden increases in da/dN are always observed when a is larger than 2 mm, fatigue cracks can then always arrest. For specimens with intermediate a_0/W (0.078 to 0.150), the results seem highly variable: sometimes the crack arrests very quickly, while in other cases the specimen may fracture after only a small number of cycles. This variability has been shown recently to be related to the variation of fibre strength after the composite is processed. For specimens with extremely short notches, no crack arrest is observed and catastrophic failure of the specimens occurs after only a small number of cycles. Similar observation on this and other systems have been made elsewhere (10,11).

In order to predict the fibre failure, the fibre stress has to be known. Several models can be used to predict the fibre stress (4,5,7). The method based on the shear-lag model needs the interfacial sliding stress to be determined, and it has been proved to be difficult to justify appropriate values(9). In this study, the fibre stress is estimated using a relatively simple method proposed by Ghosn et al. (5) assuming that the external applied stress is balanced by a bridging traction c(x). Once c(x) is known, the fibre stress, σ_f, can be estimated as σ_f/V_f. The estimated maximum fibre stress, $\sigma_{f,max}$, is listed in TABLE 1, which shows the smaller the a_0/W ratio is, the higher the $\sigma_{f,max}$ will be. Consequently, the fibres in the specimens with small a_0/W ratios are more likely to fail. This prediction is confirmed by the experimental results (Fig.4). It should be noted that Ghosn's method may often over-estimate the fibre stress and this and several other methods and models can predict the trend in crack growth resistance observed here as a function of initial crack depth (10,11).

CONCLUSIONS

The fatigue crack growth behaviour in Tiβ21s/SCS-6 under three-point bending is controlled by whether fibres fail. When the fibre stress is extremely high, many fibres fail and bridging cannot be fully developed. In this case, fatigue cracks will grow continuously leading to specimen failure. When the fibre stress is low, crack arrest occurs. Continuing fatigue under such circumstances, however, may degrade the fibre, and may sometimes result in specimen failure. When the same ΔK_0 is applied, the fibre stress in specimens with smaller a_0/W is higher. Thus, the possibility of fibre failure is also higher than in testpieces with a larger a_0/W value.

ACKNOWLEDGEMENTS

The authors would like to acknowledge the provision of research facilities in the Interdisciplinary Research Centre for High Performance Materials and the School of Metallurgy and Materials (UB). One of the authors (J.L.) would like to acknowledge the financial support from the School of Metallurgy and Materials and ORS Committee. The provision of the composite materials from Rolls Royce plc is also acknowledged with gratitude.

REFERENCES

(1) Bowen, P. and Hartley, M.V., Materials World, Vol.2, No.2, 1994, pp.66-68.
(2) Marshall, D.B., Cox, B.N., and Evans, A.G., Acta Metall.,Vol.33, 1985, pp.2013-2021.
(3) McCartney, L.N., Proc. R. Soc. Lond., Vol. A409, 1987, pp. 329-350.
(4) Davidson, D.L., Metall. Trans. A, Vol.23A, 1992, pp.865-879.
(5) Ghosn, L.J., Kantzos, P., and Telesman, J., Int. J. Fract., Vol.54, 1992, pp.345-357.
(6) Bakuchus, J.G. Jr., and Johnson, W.S., J. Composites Tech. Res., Vol.15, 1993, pp.242-255.
(7) Walls, D.P., Bao, G., and Zok, F.W., Acta Metall. Mater., Vol.41, 1993, pp.2061-2071.
(8) Begley, M.R., and McMeeking, R.M., Composites Sci. Tech., Vol.53, 1995, pp.365-382.
(9) Cox, B.N., Symposium on "Life Prediction Methodology for Titanium Matrix Composites", Hilton Head, South Carolina, March, 1994, to be published in an ASTM STP.
(10) Bowen, P., Symposium on "Life Prediction Methodology for Titanium Matrix Composites", Hilton Head, South Carolina, March, 1994, to be published in an ASTM STP.
(11) Ibbotson, A.R., "Fatigue Crack Growth in Continuous Fibre Reinforced Titanium Alloy Matrix Composites", Ph.D. Thesis, The University of Birmingham, 1993.

TABLE 1 Effects of initial notch size, a_0/W, and predicted fibre stress, $\sigma_{f,max}$, on the outcome of fatigue test carried out at an initial nominal stress intensity factor range of 17 MPa$\sqrt{m}$

a_0/W	$\sigma_{f,max}$ (MPa)	Test outcome
0.253(D)*	3049	1,386,093 crack arrest (da/dN≤10^{-8} mm/cycle), and test stopped
0.253(E)*	3052	2,118,000 crack arrest 2,361,232 crack arrest
0.239(D)	3064	3,120,000 crack arrest (da/dN≤10^{-8} mm/cycle), 3,382,106 test stopped
0.240(D)	3072	1,179,000 crack arrest (da/dN≤10^{-8} mm/cycle), but at 3,996,163 specimen fractured
0.150(D)	3141	1,304,301 specimen fractured
0.125(D)	3212	128,468 specimen fractured
0.103(E)	3329	1,248,508 crack arrest (da/dN≤10^{-8} mm/cycle), and test stopped
0.093(D)	3436	1,554,508 crack arrest (da/dN≤10^{-8} mm/cycle), 3,915,103 test stopped
0.078(D)	3578	736,009 crack arrest, and test stopped
0.048(E)	4139	146,881 specimen fractured
0.046(E)	4195	77,894 specimen fractured

* D-cut by diamond blade, E-cut by EDM

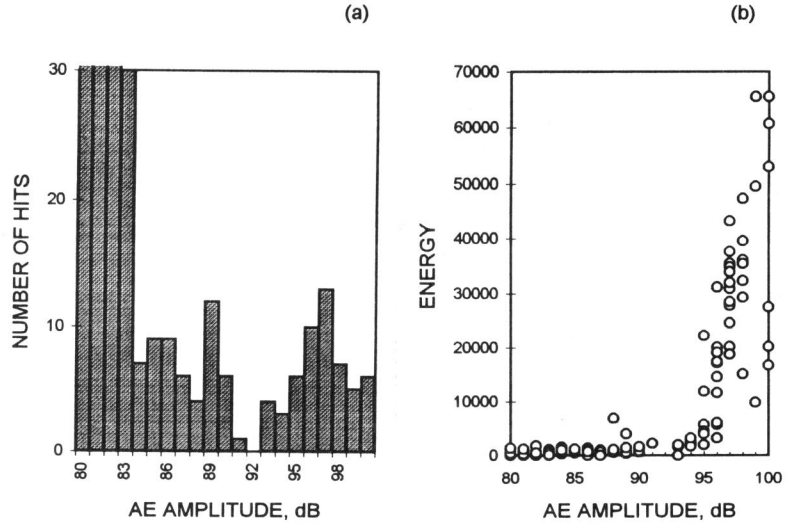

Fig.1 Typical distributions of AE amplitude(a) and energy (b) during fatigue of Tiβ21s/SCS-6

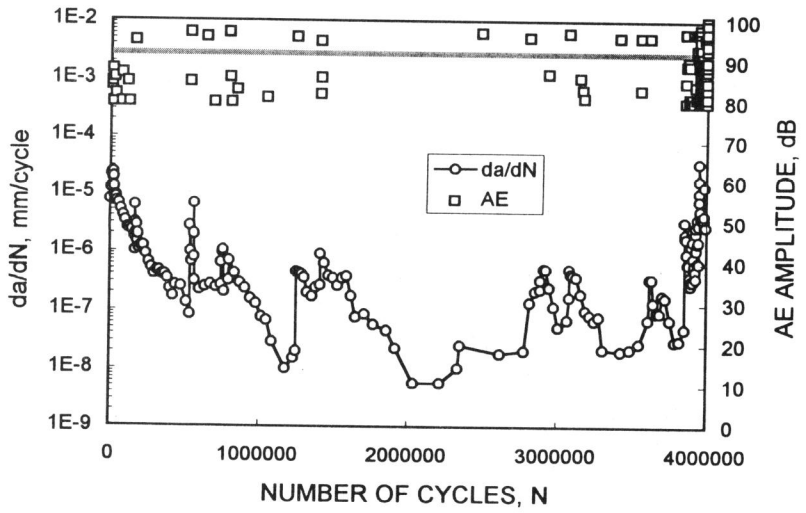

Fig.2 da/dN and AE amplitude , versus number of cycles. (a_0/W=0.240)

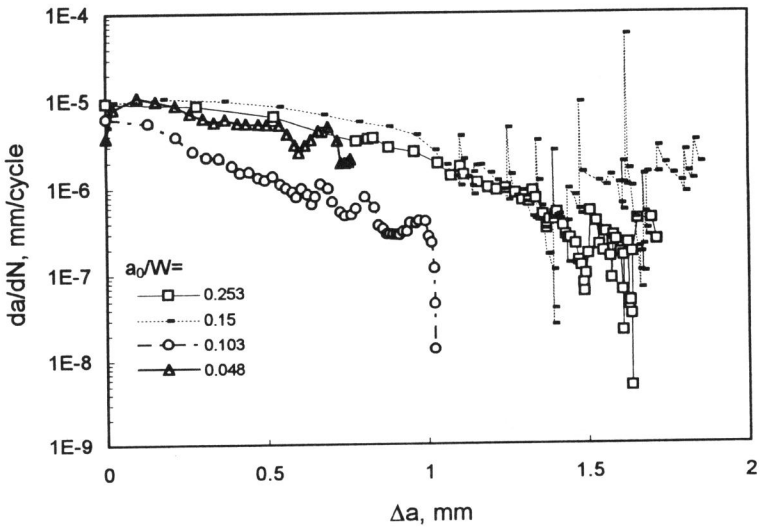

Fig.3 Fatigue crack growth rate, da/dN, versus crack growth distance, Da, in specimens with different a_0/W ratios

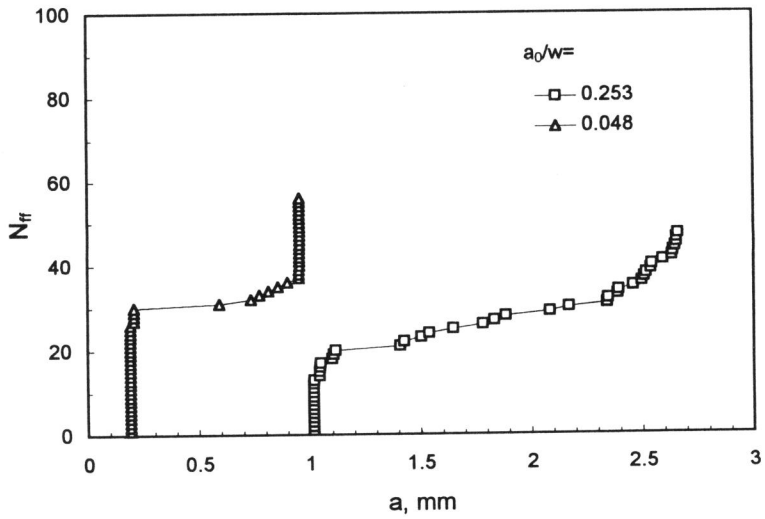

Fig.4 Number of fibre failures, N_{ff}, versus crack growth distance, Da.